Journal Pre-proof

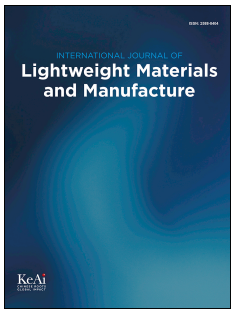

Wood flour / ceramic reinforced Polylactic Acid based 3D - printed functionally grade structural material for integrated engineering applications: A numerical and experimental characteristic investigation

Arunkumar Thirugnanasamabandam, Prabhu B., Varsha Mageswari, Murugan V., Karthikeyan Ramachandran, Kumaran Kadirgama

PII: S2588-8404(24)00080-5

DOI: https://doi.org/10.1016/j.ijlmm.2024.08.003

Reference: IJLMM 336

To appear in: *International Journal of Lightweight Materials and Manufacture*

Received Date: 27 May 2024

Revised Date: 1 July 2024

Accepted Date: 14 August 2024

Please cite this article as: A. Thirugnanasamabandam, B Prabhu, V. Mageswari, V Murugan, K. Ramachandran, K. Kadirgama, Wood flour / ceramic reinforced Polylactic Acid based 3D - printed functionally grade structural material for integrated engineering applications: A numerical and experimental characteristic investigation, *International Journal of Lightweight Materials and Manufacture*, https://doi.org/10.1016/j.ijlmm.2024.08.003.

Wood flour / ceramic reinforced Polylactic Acid based 3D - printed functionally grade structural material for integrated engineering applications: A numerical and experimental characteristic investigation

Arunkumar Thirugnanasamabandam[1,2]*, Prabhu B[2], Varsha Mageswari[3], Murugan V[1], Karthikeyan Ramachandran[4], Kumaran Kadirgama[2,5]

[1]Centre for Additive Manufacturing, Chennai Institute of Technology, Chennai, India.

[2]Centre for sustainable materials and surface metamorphosis, Chennai Institute of Technology, Chennai, India.

[3]Department of Biomeical Engineering, Chennai Institute of Technology, Kundrathur, Chennai, India.

[4]Department of Aerospace and Aircraft Engineering, Kingston University, London, SW15 3DW, United Kingdom.

[5]Faculty of Mechanical & Automotive Engineering Technology, Universiti Malaysia Pahang Al-Sultan Abdullah, 26600, Pekan, Pahang, Malaysia

Corresponding author: * arunkumar.t@citchennai.net

Wood flour / ceramic reinforced Polylactic Acid based 3D - printed functionally grade structural material for integrated engineering applications: A numerical and experimental characteristic investigation

Abstract

Recently, efforts have been done to capitalize on the potential of multidisciplinary research in order to produce unique features in polymer technology. To improve its physical and chemical properties for any intended use, the most promising Polylactic acid (PLA) has recently been copolymerized using other polymeric or non-polymeric components. This investigation aims to employ the material extrusion (MEX) process to develop a new functionally grade structural material (FGSM) by alternate layer deposition of wood flour reinforced PLA (WPLA) and ceramic reinforced PLA (CPLA). The mechanical properties of the printed laminates are examined using tensile, compression and three point bend tests. The microscopic investigation is used to assess fracture morphologies. A numerical simulation is also performed using ABAQUS under standardized parametric settings to investigate the mechanical behaviour of the laminates. The experimental and numerical results are consistent, with a deviation about ~1 %. The tensile, compressive, and flexural strength of the newly developed FGSM are 61.39, 95.4, and 107.8 % higher than those of WPLA printed laminates. Furthermore, the acquired mechanical behaviour results are merely comparable to those of CPLA printed laminates. DSC thermograms demonstrate that FGSM has a better glass transition temperature (66^{o}C) and a cold crystalline temperature (87.63^{o}C), which contributes to its thermal stability. Overall, the newly developed FGSM might be considered a viable alternative, mechanically strong, and less expensive polymer composite material for structural built applications in any engineering and related fields.

Keywords: *WPLA and CPLA polymers; Functionally Grade Structural Material; MEX; Mechanical behaviour; Thermal properties.*

1. Introduction

1.1. Background and motivation

Technological developments have been revolutionizing raw materials which can be effectively utilized in polymer technology. Because of the environmental impact of petrochemical-derived plastics, plant-based alternatives are a potential option. Biodegradable

biopolymers such as Polylactic acid (PLA), Polyamide (PA), and Polycaprolactone (PCL) can be used as biodegradable plastics for a variety of purposes. PLA, a popular biopolymer, is derived from corn sugar and tubers such as cassava [1]. It has applications in a wide range of industries, including biomedicine, textiles, electronics, and packaging. It's hard and brittle. PLA serves as an effective reinforcement matrix, allowing materials such as wood, carbon, clay, and ceramic to be easily reinforced with PLA [2-4]. PLA is commonly used in additive manufacturing (AM) due to its superior printability.

The AM process can produce prototypes by layer-by-layer deposition of materials. Traditional production procedures have drawbacks in terms of cost, material utilization, and equipment management [5]. The AM approach, on the other hand, reduces these limitations while also making it easier to create complicated geometric designs [6]. The AM process is used in a variety of industries, including aerospace, automotive, biomedical, and architectural [7]. Furthermore, it might be used in a variety of applications due to its ability to enable highly customized production, reduce material waste, and keep production costs low [8]. It is an environmentally friendly production technology as it is easy to operate, uses bio-based polymers as raw materials, and provides superior energy and environ-economic performance [9]. Parts fabricated using AM processes help to increase internal strength while reducing total mass. In the biomedical industry, the AM process has been employed to create polymeric scaffolds [10, 11] and titanium implants to replace skeletal bones [12, 13]. Tissue engineering is also an AM process in which live tissues are additively produced and then implanted. New materials development, particularly polymer and metal-based composite materials and their structures, is inextricably tied to the evolution of AM process [14].

AM fabrication processes include laser sintering, powder bed fusion, material extrusion (MEX), and binder jetting [15]. According to ISO 52900, the term material extrusion (MEX) is used for fusion deposition modelling (FDM). MEX process is the most widely used of these due to its inexpensive cost, design flexibility, and ability to build structures with complicated geometries rapidly [16]. Furthermore, the production of thermoplastic materials using the MEX process is widely suitable to a variety of applications [17]. The MEX process is more favorable, although it has a detrimental impact on surface quality and dimensional accuracy [18, 19]. The proper choice of printing settings is essential because they influence the mechanical and surface roughness behaviours of prints [20]. Polymeric structures can be produced with pre-set

parameters by feeding the design model into the machine [21]. The AM approach via MEX process offers greater benefit for fabricating polymer-based prototypes such as functionally graded structural material (FGSM).

PLA is a viable biopolymer material for building structures in a variety of applications due to its physical and chemical properties. FGSM is a composite structure made up of two or more distinct materials [22, 23]. Additional studies on PLA-based FGSM is being carried out in order to create a more efficient new structured material through alternate layer deposition of various filler-reinforced PLA for improving its mechanical interactions at each layer interface and to investigate its suitability for any integrated engineering application. FGSM with strong thermal gradient resistance is used to manufacture spacecraft bodies and rocket engine components. FGSM has a greater advantage for replacing bones and teeth. Their involvement extends to automobile, energy generation, electrical, and optical electronics fields. In this context, researchers in this field are motivated to investigate the usage of innovative PLA-based composites for producing FGSM structures and determining their suitability for end applications.

PLA-based composites with various fillers used as a filament for polymer structures are more attractive [24–27]. Wood flour reinforced PLA (WPLA) is lightweight and biocompatible. However, the mechanical properties of 3D printed composites may be influenced by the size of wood particles [28] and the chemical treatment of wood fibers [29, 30]. Ceramic-reinforced PLA (CPLA) offers improved compatibility and compressive strength. Furthermore, it is used to create a more wear-resistant material for medical devices, implants, and orthoprosthetics. Previous numerical and experimental investigations on developing composite structures with bio-polymers and/or wood/ceramic particles have been comprehensively assessed to examine their process considerations and outcomes.

The researchers statistically optimised the MEX process parameters to improve the ultimate strength, young's modulus, and flexural strength of PLA-based polymer structures [31–33]. Khosravani et al. [34] found that the MEX technique was a viable option for developing 3D structured composites and investigated the fracture and structural performance of adhesively bonded 3D-printed PETG single lap joints using various printing parameters, such as raster angles (0, 45, and 90^{o}), raster widths (0.75 and 1 mm), and layer thicknesses (0.2 and 0.5 mm). The study concluded that reduced layer thickness (0.2 mm), raster width (0.75 mm), and raster

orientation (0^o) were viable printing parameters for producing 3D printed adhesively joined components with improved strength and structural performance.

Khosravani et al. [35] investigated the effects of surface treatment on 3D printed ABS-based dog-bone structures with varied raster angles (0.45 and 90°) and infill density (100%). The findings indicated that chemical treatment might be utilized to improve the surface quality of 3D-printed specimens; nevertheless, lowering surface roughness affects the mechanical and structural performance of the printed parts. Fountas et al. [36] employed the RSM technique to optimize the effect of nozzle temperature and layer thickness on surface roughness for PLA and WPLA-based 3D printed samples. The results revealed that PLA and WPLA-based 3D printed specimens had better surface roughness (~2.220 and 8.812 μm, respectively). The optimal nozzle temperatures of 180 and 220^{o}C, as well as layer thicknesses of 0.1 and 0.18 mm, were determined to be adequate for printing PLA and WPLA-based specimens.

Fountas et al. [37] optimized the printing parameters for WPLA-based 3D printed parts, including layer thickness, printing speed, nozzle temperature, and raster angle. It was discovered that raster angle deposition (0°) and nozzle temperature (180°C) had the greatest influence on the ultimate tensile strength of prints. Ecker et al. [38] investigated the mechanical and water absorption properties of PLA and WPLA-based composites produced by 3D printing and injection moulding techniques. Following the water absorption tests, the injection moulded part absorbed greater impact energy. The tensile characteristics of the parts produced using the two targeted techniques were lowered after water absorption evaluation. The findings reveal that mechanical properties of 3D printed parts change following water absorption, implying that proper selection of polymer composites and surface treatment are essential for producing ideal structures for any application, particularly bio-medical implants.

Regarding, Jubinville et al. [39] studied the combined effect of chemical wood alteration and PLA recycling/maleation on tensile and water absorption capabilities. The results showed that chemically treated wood particles and the PLA meleation process increased the composite structure's water repellent and dimensional stability while retaining its tensile strength and modulus. Travieso-Rodriguez et al. [40] examined the fatigue behavior of 3D printed composites based on PLA and Timberfill wood particles, considering printing parameters such as layer height, infill level, infill pattern, extrusion velocity, and nozzle diameter. The results showed that the printing parameters of honeycomb pattern, infill density (75 %), nozzle diameter (0.7 mm),

and layer height (0.4 mm) were recommended to improve the fatigue life of the WPLA-based printed part.

Zhang et al. [41] studied the tensile and flexural properties of PLA grafted with maleic anhydride, as well as its thermal stability, and compared the results to those of PLA and WPLA-based injection moulded samples. The results showed that PLA grafted with maleic anhydride functioned as an interfacial compatibilizer, increasing the composites' tensile and flexural strengths by 9 and 6 %, respectively, while lowering water absorption. Guessasma et al. [42] investigated the mechanical behaviour of a WPLA-based 3D printed object using both experimental and numerical methods at printing temperatures ranging from 210 to 250^{o}C. The results showed that as the temperature was raised, the printed part's tensile strength gradually increased. The results show that WPLA could be used in applications where texture is more important than tensile strength.

The use of ceramic particles as reinforcements to PLA / WPLA can improve mechanical properties as the ceramic particles increase stiffness and strength while also improving load-bearing capacity. Bio-ceramic materials, in particular, are ideal for the biomedical industry due to their exceptional biocompatibility and robustness. In general, natural hydroxyapatite (NHA) and bio-active glasses are appropriate bio-ceramic materials for MEX-based artificial scaffold development. 3D printing of pure NHA using the MEX process may not be feasible. Pre-processing with an adhesive binder (PVB) and a plasticizer (PEG) is recommended to soften the base NHA and form the desired shape. Alternatively, suitable ceramic fillers equivalent to NHA are added to PLA polymer via melt blending to make composite filament for the development of artificial bio-structures in the biomedical field [43].

Thomazi et al. [44] studied the effects of integrating NHA, Al_2O_3, and ZrO_2 particles into PLA to determine their potential for producing mimic cortical bone in anthropomorphic simulators. The findings demonstrated that PLA with 6 wt. % ZrO_2 composite-based printed parts gave better results in yielding Hounsfield Unit, which was merely comparable to mimicking cortical bone. In contrast, PLA with NHA / Al_2O_3 composites had shown no significant advantage over pure polymers in soft tissue applications.

Liu et al. [45] studied the mechanical properties of printed parts utilizing ceramic, wood, carbon, and aluminum metals based PLA composites with different build orientations (on-edge, flat, and upright) and raster angles (0, 90 and ±45^{o}). Ceramic-based PLA samples produced with

a flat orientation and a +45^{o} raster angle showed a maximum tensile modulus of 1.05 GPa and a maximum flexural modulus of 4.6 GPa. The authors discovered that bio-ceramic materials can be utilized in bone therapy and to repair many types of bone deformities [46]. Mohankumar et al. [26] studied the mechanical properties of 3D-printed structural-grade PLA/ceramic reinforced PLA materials. It was discovered that structurally graded materials had superior mechanical and impact properties than the pure PLA based structure.

1.2. Novelty and objective

Existing research suggests that the MEX approach is most suited to producing intricate and desirable 3D printed structures with improved strength and dimensional accuracy using various polymer composites. Notably, wood flour-reinforced polymer composites have emerged as a potential material to produce lightweight printed composites with superior tensile and flexural properties. However, ceramic fillers could be used to improve strength properties while balancing the optimum properties of wood flour-reinforced polymer composites, which have become increasingly prevalent in industrial applications. As a result, further research is required to assess the strength properties of wood flour/ceramic reinforced composite structures. Furthermore, most studies have concentrated on bulk layering of functionally graded polymer-printed laminates. However, there has been limited progress in developing functionally grade structural materials via alternate layer deposition of various filler-reinforced PLA, which has to be envisioned to improve mechanical interactions at each layer interface of a wood flour and ceramic filler-reinforced polymer composite and investigate its suitability for any integrated engineering applications. Hence, research progress is needed to ascertain the mechanical, thermal, and microstructural properties of 3D-printed alternate layered wood flour and ceramic-reinforced polymer laminates. This comprehensive investigation is beneficial in utilizing the potential functionalities of WPLA / CPLA polymer composites for developing a stable FGSM laminate for any integrated engineering applications, and it intensively paves the way for researchers to conduct a progressive research on developing more efficient FGSM structures for lightweight material manufacturing.

The main objective of this research is to evaluate the mechanical, microstructural, and thermal properties of functionally graded structural material (FGSM). FGSM is produced via alternate layer deposition of pure wood flour and ceramic-reinforced PLA polymer filaments by the MEX process utilizing appropriate printing conditions suggested in the

related literatures. Furthermore, using the same printing process parameters, wood flour / ceramic-reinforced PLA polymer filaments (WPLA/CPLA) - based laminates are produced to serve as comparison materials to the FGSM laminates. Furthermore, differential scanning calorimetry (DSC) has been utilized to examine thermal properties of 3D-printed laminates. Finite element simulation analysis via ABAQUS is used to validate the experimental results on mechanical behaviours. Statistical analysis is carried out by determining standard deviation and co-efficient of variation on experimental and numerical study results for assessing their repeatability. Furthermore, scanning electron microscopy (SEM) is used to perform fractography analysis of the fractured FGSM laminates.

2. MATERIALS AND METHODS

2.1 Materials

Wood flour reinforced PLA (WPLA) and Ceramic reinforced PLA (CPLA) polymers are utilized as feedstock due to their biocompatibility, better printability and providing stable mechanical and thermal performance. The FGSM is produced utilizing the MEX process due to its cost-effectiveness, ease of usage, minimal waste produced, massive build volume, and eco-friendliness. This study utilizes commercial-grade, PLA Wood and ceramic composite filaments (~Φ1.75mm) purchased from the reputed WOL3D, India. The filaments comprise ~70 % PLA and ~30 % of wood flour / alumina particles, resulting in composite filaments. The density of filaments is 1.25 ± 0.05 and 2.53 g/cm^3, respectively.

2.2 3D printing process

The fabrication of FGSM is carried out using the PRATHAM 3.0 MEX 3D printer, featuring a greatest build volume of 300×300×300 mm³ and a tolerance of ± 0.1 mm. The silicone heated build platform enhances proper adhesion between the bottom layer and the base to prevent material warping during the fabrication process. The CAD drawing of the proposed FGSM is designed in CATIA V5 R20 and exported as a stereolithography (STL) file. Then the STL file is imported into Ultimaker Cura 5.1.1 slicing software, where process parameters for the print are clearly specified.

It has been established that reinforced polymers have superior characteristics and greater melting temperatures than pure polymers. Regarding, process parameters are chosen to be

suitable for developing FGSM using the targeted polymer composites via alternate layer deposition. These parameters are obtained by trial-and-error iterations, involving variations in nozzle temperature (200 to 230°C), bed temperature (50 to 70°C), and printing speed (10 to 30 mm/sec). A nozzle temperature of 210°C produces a steady flow of printed samples with a good surface finish. This temperature is slightly higher for WPLA filament, it is beneficial, particularly when coupled with a brief dwell time, which facilitates inter-layer diffusion and thus increases bond strength. Maintaining the bed temperature at 60°C ensures optimal bonding between composite layers and the build platform. Furthermore, air gaps between rasters are reduced at a printing speed of 20 mm/sec. The process parameters utilized in this study to develop the 3D printed laminates are given in **Table 1**.

Table 1 Process parameters utilized

Process parameters	**Values**
Layer pattern	Line
Layer Height (mm)	0.2
Orientation of layer (^{o})	0
Infill density (%)	100
Printing speed (mm/s)	20
Printing temperature (^{o}C)	210
Printing bed temperature (^{o}C)	60

After setting the process parameters, the associated G-codes are developed. Then, it is fed into the machine to produce FGSM using alternate layer deposition of WPLA and CPLA filaments. An appropriate adhesive is sprayed over the silicon heated bed to ensure good adhesion between the base layer and the bed, allowing the sample to be orientated without warping. PLA is printed as a base support layer to enhance bonding with the bed. The suggested WPLA and CPLA fillers are then printed via alternate layer deposition, with each layer having a consistent thickness of 0.2mm. The 2 mm thick printed FGSM, shown schematically in Fig. 1, is composed of alternate 5 layers of WPLA and CPLA polymers. The resulting sample is allowed to cool for improved layer-to-layer bonding.

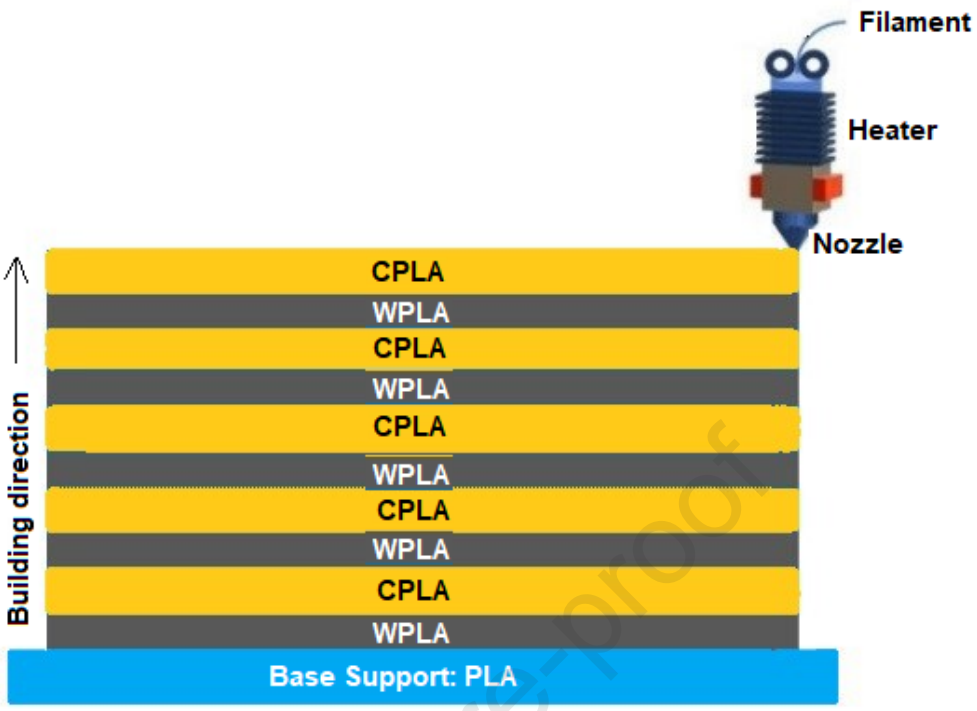

Fig. 1 Schematic front view of the FGSM laminate

2.3 Characterization

The associated samples for characterization from the printed laminates are prepared in accordance with ASTM standards, including ASTM D3039 for tensile, ASTM D695-6641 for compression, and ASTM D790 for flexural [27], resulting in the creation of three sets of testing samples (three samples per set, for a total of 9 samples) via water jet machining. The mechanical characteristics of the prepared samples are evaluated using the Universal Testing Machine (Model: Tinius Olsen). The UTM with a maximum load capacity of 50 kN is used to evaluate the strength and slenderness of the printed laminates. The UTM is run in crosshead displacement mode, with a strain rate of 1 mm/min, until the samples fracture. The thermal stability of all printed laminates is evaluated using Differential Scanning Calorimetry (NETZSCH DSC 214). Each sample is heated from 30 to 250°C at 10°C per minute to determine its glass transition, cold crystalline and melting temperatures. Scanning electron microscopy (Model: Carl Zeiss SIGMA) examines the morphology of tensile fractured samples. The final reading of each characterization test is derived as the average of their three standardized testing results. The tensile and compressive properties of WPLA, CPLA, and FGSM printed laminates are validated using numerical simulation with ABAQUS.

3. Results and Discussion

3.1. Three point bend test

Flexural strength is an ability of a material to withstand bending force applied perpendicular to its longitudinal axis. The three point bend (TPB) test is used to measure the flexural strength of WPLA, CPLA and FGSM printed laminates. A span length of 3 cm and a steady strain rate of 2 mm/min are considered. Fig. 2(a, b and c) depicts the physical behaviour of the 3D printed laminates during loading at TPB test.

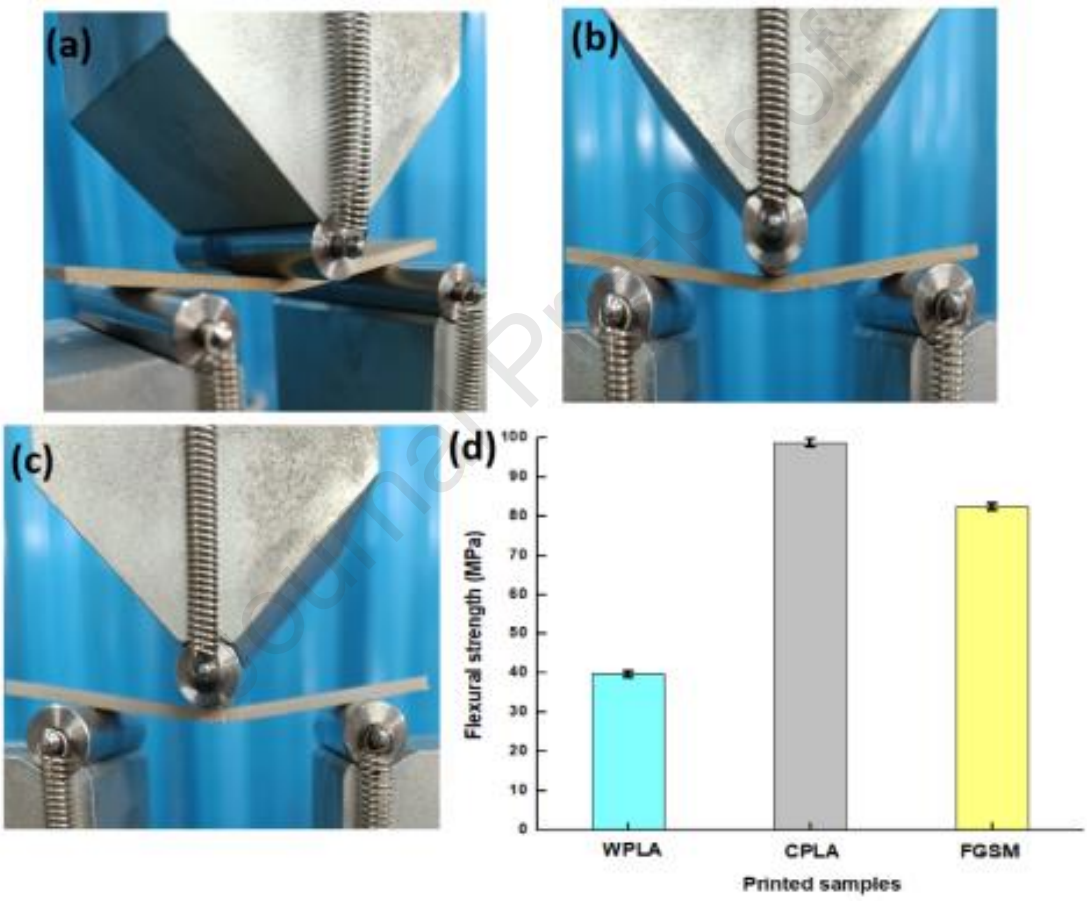

Fig. 2 TPB study on the printed laminates of (a) WPLA, (b) CPLA, (c) FGSM and their (d) flexural strength

Fig. 2(d) depicts the consolidated results of the achieved flexural strength of the printed laminates. Flexural strength of the FGSM-based laminate is greater (83.35 ± 0.9 MPa) than that of the WPLA-based sample (40 ± 1.08 MPa). The FGSM has greater flexural strength (107.8 %)

than the WPLA-based laminate, making it a suitable alternative material for any engineering applications that require WPLA.

The developed FGSM's flexural strength is declined by 16.39 % than that of CPLA based sample (99.7 ± 1.1 MPa). This is due to the contribution of weaker WPLA material in the FGSM laminate. However, the proper inner bonding between the WPLA and CPLA and no more occurrence of delamination in the fractured zone are achieved in the first-time experimental investigation on the development of FGSM laminate structures. The FGSM laminates based on wood flour / ceramic reinforced polymers have improved bonding properties due to improved interfacial adhesion between the layers of the targeted polymers. The printing process and its associated parameters promote better inter-layer bonding and inter-diffusion during each layer's printing. Furthermore, the solidification time before printing each layer has a favourable impact on the building quality of alternative layer deposition. This process efficiently transported heat to subsequent layers, lowering the possibility of unanticipated deformation in the bottom layer [47]. It is worth noting that the load concentration at the sample's centre, where failure occurred, did not cause delamination in the fracture zone. This finding lends support to the contention that FGSM has strong bonding strength. As a result, the produced FGSM has superior and comparable flexural properties than WPLA and CPLA-based printed laminates, respectively. The results of this study are reviewed and compared to those of other studies that have used various fillers to increase the flexural strength of 3D printed laminates. Parikh et al. [48] investigated the flexural response of 3D printed laminates utilizing PLA/wood polymer, and they generated a mechanically stable laminate with a flexural strength of 36 MPa using 22 wt. % wood dust-filled PLA filaments, which is 10% lower than that of this work utilizing ~70 wt. % of PLA and ~30 wt. % of PLA/Wood polymers. Choudhary et al. [49] utilized PLA-based bio-ceramics (Al_2O_3 and Yttria Stabilized Zirconia [YSZ]) for examining their mechanical characteristics. The printed laminates exhibited tensile, compressive, and flexural strength of 30.44, 55.2, and 83.73 MPa respectively. The obtained flexural strength of this study is 19.1 % higher than that of the studies utilized PLA/Alumina polymers.

3.2 Tensile property study

Tensile property characteristic studies are performed on developed samples in order to comprehend their elongation and associated tensile strength. Fig. 3(a, b) depicts the physical

behavior and obtained tensile strength of the printed samples respectively. The tensile strength of the FGSM laminate is 57.02 ± 0.6 MPa, which is 61.39 % more than that of the WPLA based sample (35.33 ± 0.9 MPa). The results show that the weaker WPLA material is properly reinforced with CPLA, allowing it to endure the maximum tensile load. This enhancement can be due to the greater interfusion of layers in the multilayer structure, which promotes higher tensile characteristics. The increased tensile strength is also attributable to the bonding mechanism that happens between materials during layer deposition, which includes a short break before printing each layer in a semi-molten condition. The combination of ceramic particles serving as nucleating agents and a moderate cooling rate improves the crystallinity of the FGSM laminate.

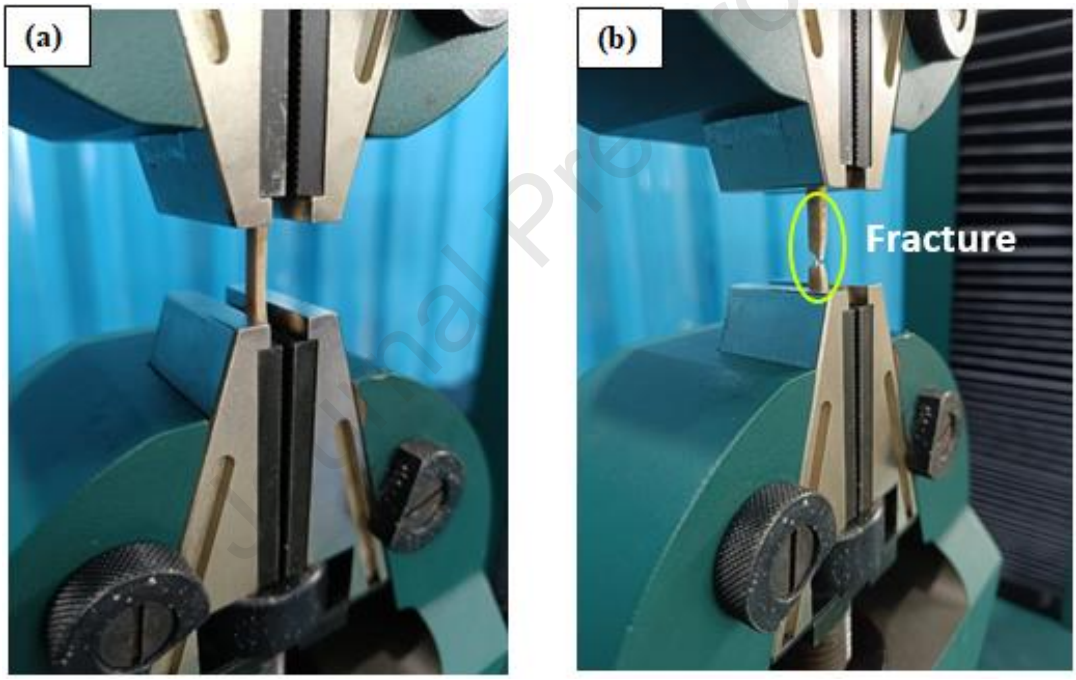

Fig. 3(a) Physical behaviour of FGSM laminates during tensile study
(a) before (b) after loading

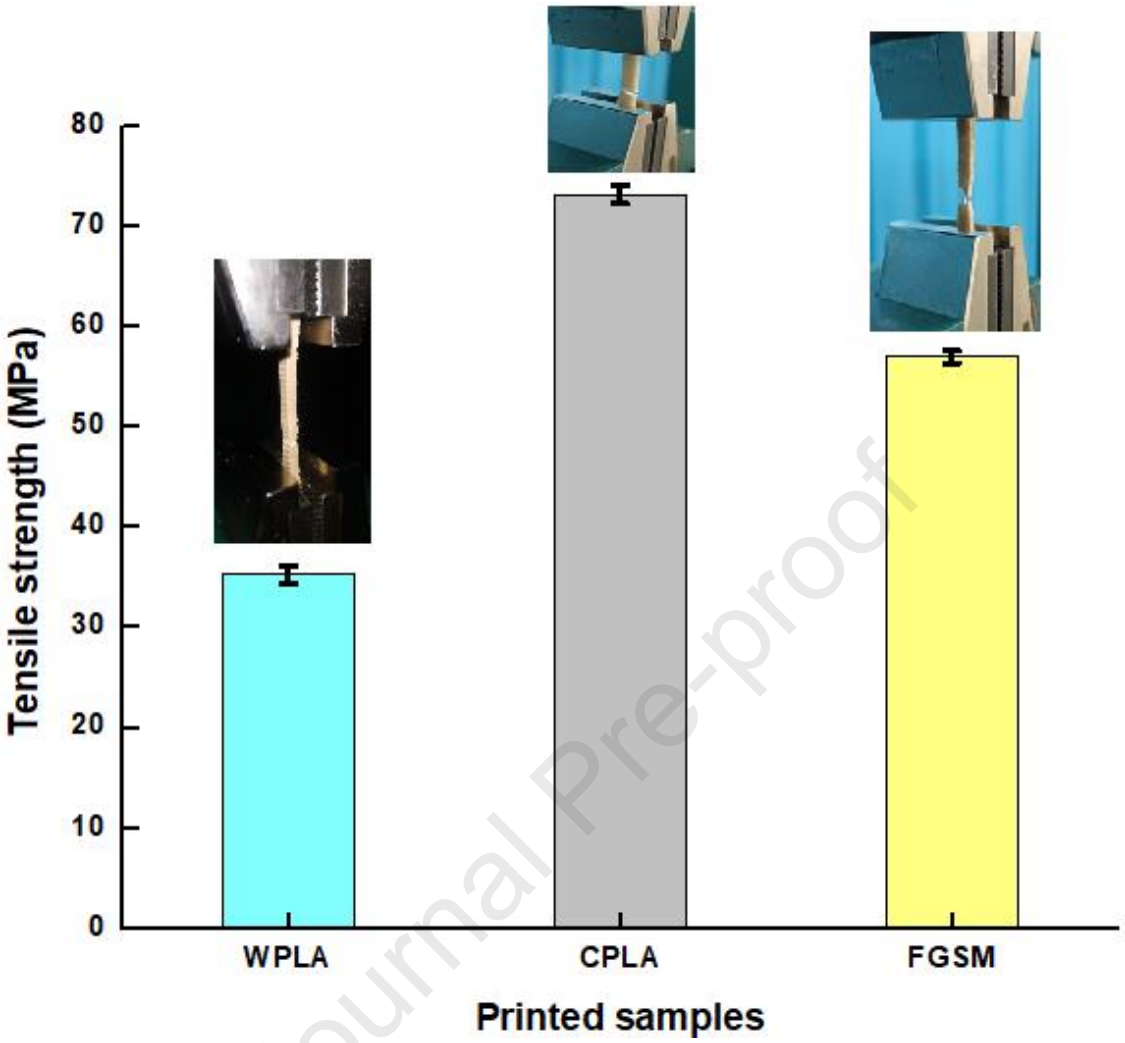

Fig. 3(b) Tensile strength of the printed laminates

Furthermore, the layer orientation (0^o) contributes to yield of higher tensile strength due to its layers are exactly parallel to the load applied. In this orientation, the layers are more likely to link together, resulting in a continuous and homogeneous structure that can withstand higher tensile stresses before breaking. This phenomenon is supported to enhance elongation percentage of the developed FGSM laminate. The elongation percentages of the WPLA and FGSM samples are 4.41 ± 0.5 and 5.78 ± 0.4 %, respectively. An improved elongation (31.1 %) supports to absorb more tensile stress. Because of the relative presence of the weaker WPLA material, the FGSM laminate exhibits lower tensile strength than the CPLA-based sample. Tensile strength is

reduced by 22.1 % in the FGSM laminate compared to the CPLA-based sample (73.2 ± 0.9 MPa).

Arunkumar et al. [50] investigated the mechanical properties of PLA and carbon reinforced PLA-based alternative layered 3D printed laminates. The results revealed that carbon reinforced PLA polymer was used to develop a laminate with a higher tensile strength (56.28 MPa), which is lower than the tensile strength (57.02 MPa) obtained in this study, due to the effect of ceramic particles, which positively encourage nucleation behaviour on improving the crystallization rate of the composites during printing, thereby improving interfacial bonding between the alternate layers of polymers and thus support to improve its tensile strength. Similar kind of research works utilized PLA/Wood and PLA/carbon to produce and investigate mechanical properties of 3D printed multi-layer composite laminates [51]. The produced laminates resulted tensile strength of 51.47 MPa, which is much lower than that of the laminate produced this study due to an impact of strong ceramic particles. Gurusamy et al. [23] investigated the effect of PLA and PLA/Wood on the development of mechanically stable multi-layered structural materials at different raster angles (0, 45, and 90^{o}). The results demonstrated significant differences in the mechanical characteristics of multi-layered materials depending on raster angle. The produced multi-layered laminates had a maximum tensile strength of 46.45 MPa at a raster angle of 0^{o}. The obtained result is 22.57 % lower than the laminated sample produced in this study using alternate layer deposition of PLA/wood and Ceramic reinforced PLA, confirming the potential of the selected polymer composites and printing process parameters in producing more mechanical and thermal stable laminates for the suitable structural engineering applications.

The related stress-strain curve of the printed samples is depicted in **Fig. 3(c).** Though the FGSM laminate has a lower tensile strength, its appropriate physical bonding makes it a comparable material to more structurally bonded CPLA. An increase (8.2 %) in the elongation percentage of the FGSM laminate with that of the CPLA based sample (5.34 ± 0.4 %) demonstrates that the FGSM sample absorbs and withstands its permissible loads, confirming potentiality in related applications and rendering it a comparable material to the CPLA based sample.

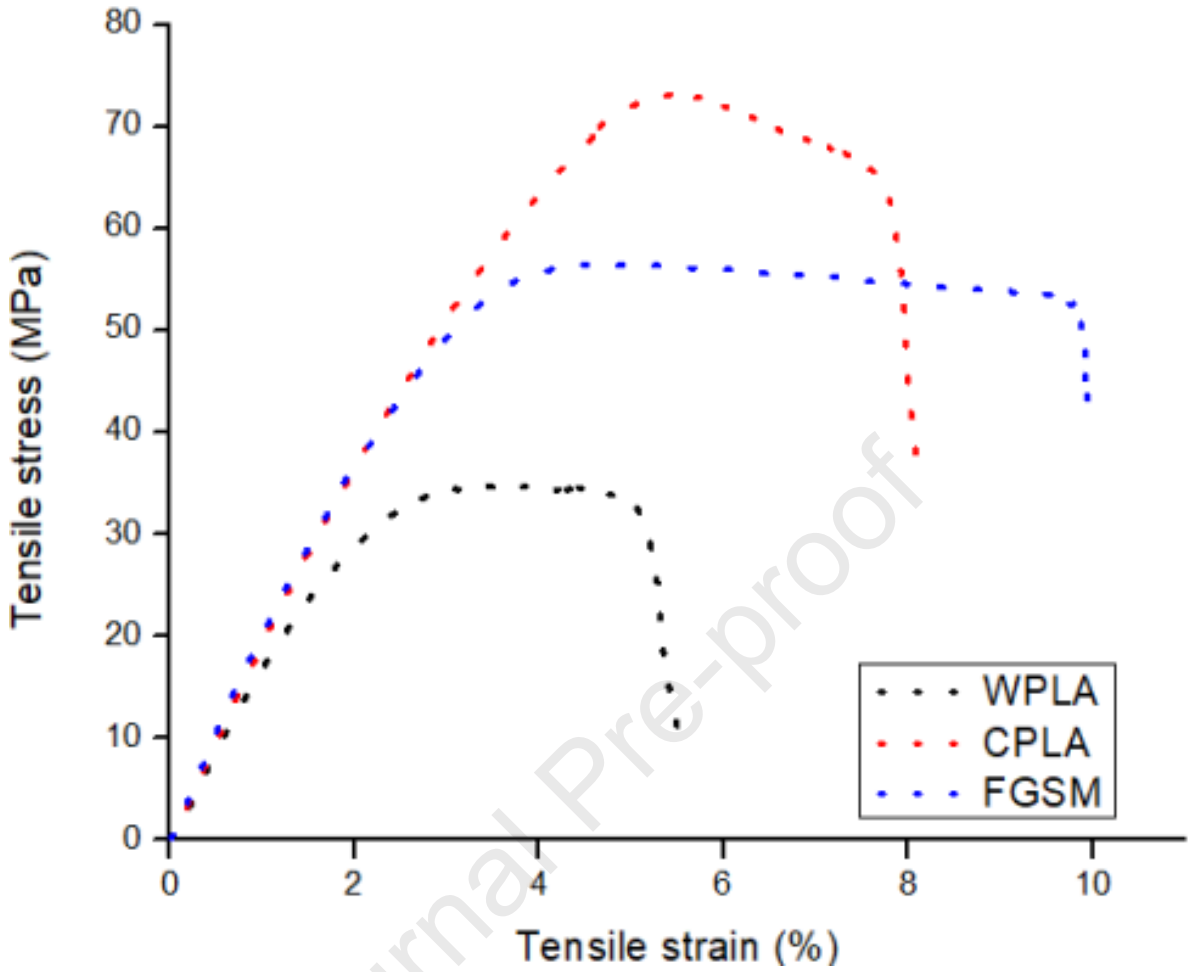

Fig. 3(c) Tensile stress – strain curve of the printed laminates

3.3 Compression test

Compression testing is an important aspect of polymer characterization. It provides information on a polymer's compressive strength and compressive yield strength, which are significant in determining a polymer's load-bearing capability and applicability. All the developed samples are insisted for compression testing. Fig. 4 depicts the experimental view and the obtained compressive strength of the WPLA, CPLA, and FGSM-based printed laminates. The compressive strength is obtained by 39.67 ± 1.3 MPa, 98.4 ± 1.6 MPa and 77.54 ± 1.5 MPa, respectively, for the WPLA, CPLA and FGSM based laminates. The CPLA concentration in the FGSM laminate increases its compressive strength. The compressive strength of the FGSM laminate is 95.4% higher than that of the WPLA-based sample.

This improvement is due to ceramic particles reinforcing polymers, which resist deformation and absorb more energy during compression loading [52]. Palaniyappan et al. [53] produced 3D printed laminates with 50% single-gradient PLA and 50% walnut shell reinforced PLA. A maximum compressive strength of 63.68 MPa was achieved, which is 21.7% lower than that of the laminates produced in this study, which explores the potential of FGSM design configuration, targeted polymers and process parameters used. However, the weaker and flake morphology structured WPLA in the produced FGSM based laminate may not be adequate to endure maximum strength. When compared to CPLA, the compressive strength of the FGSM laminate is reduced by 21.1%. However, a proper bonding between WPLA and CPLA aids in lowering the tendency of buckling effect under compressive load and thus allow it to withstand its permissible load, making it a viable composite material for any integrated engineering applications.

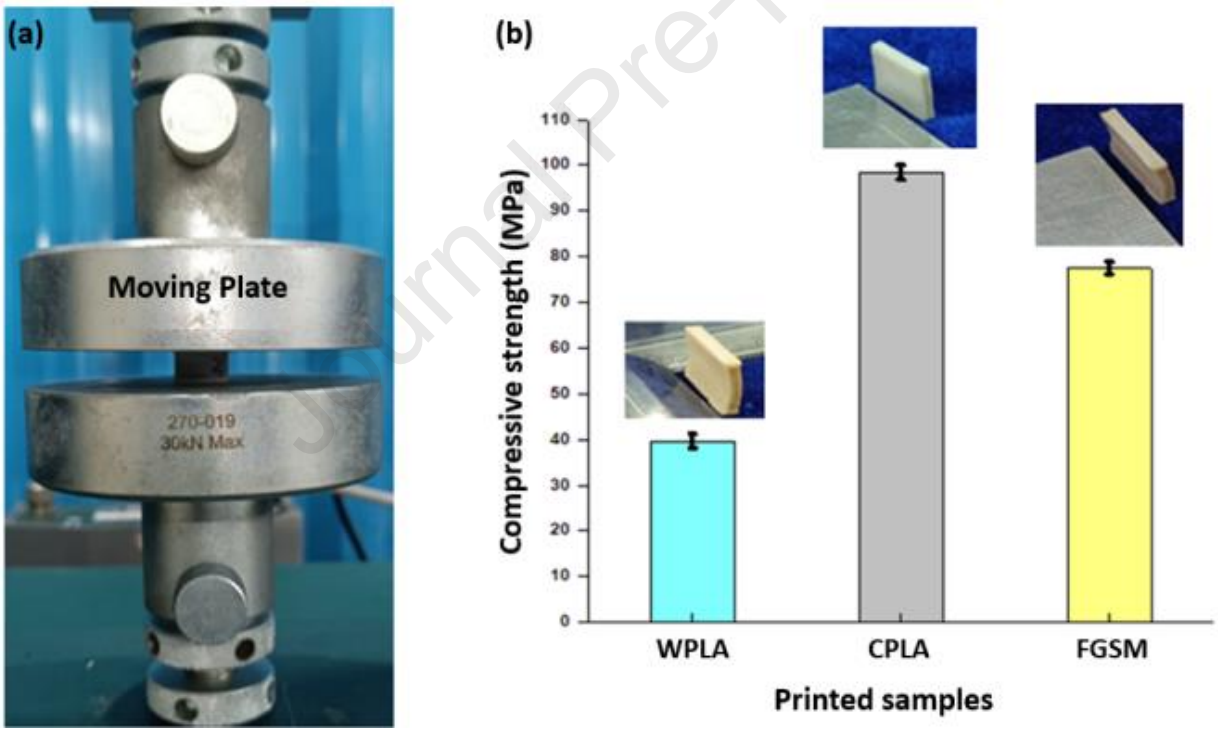

Fig. 4 Compression study of the printed laminates (a) Experimental view
(b) Obtained compressive strength

3.4 Statistical analysis of experimental study results

Experimental studies on tensile, compressive, and flexural strengths are statistically validated by determining the standard deviation and coefficient of variation to assess reliability of the results. Three sets of samples of WPLA, CPLA, and FGSM printed laminates are insisted for mechanical characterization under same operating conditions. The collected data are statistically assessed, and the corresponding values are shown in Table 2. Where σ_t, σ_c, and σ_f represent experimental tensile, compressive, and flexural strength, respectively. σ_{tdev}, σ_{cdev}, and σ_{fdev} represent the standard deviation of experimental results on tensile, compression, and flexural strengths, respectively. $\nu_{\sigma t}$, $\nu_{\sigma c}$, and $\nu_{\sigma f}$ are the coefficients of variation on experimental tensile, compression, and flexural strengths, respectively. ε_t represents the elongation percentage of tensile sample. $\varepsilon_{\varepsilon tde}$ and $\nu_{\varepsilon t}$ represents the standard deviation and co-efficient of variation of sample elongation during tensile testing. The acquired statistical results confirm the repeatability of the readings obtained in tensile, compressive, and flexural studies.

Table 2 Statistical analysis of experimental study results

Samples	Tensile strength						Compressive strength			Flexural strength		
	σ_t	σ_{tdev}	$\nu_{\sigma t}$	ε_t	$\varepsilon_{\varepsilon tde}$	$\nu_{\varepsilon t}$	σ_c	σ_{cdev}	$\nu_{\sigma c}$	σ_f	σ_{fdev}	$\nu_{\sigma f}$
	[MPa]	[MPa]	[%]	[%]	[%]	[%]	[MPa]	[MPa]	[%]	[MPa]	[MPa]	[%]
WPLA	35.33	0.90	2.54	4.41	0.50	11.28	39.67	1.3	3.27	40	1.08	2.7
CPLA	73.2	0.90	1.22	5.625	0.55	9.77	98.4	1.6	1.62	99.7	1.1	1.1
FGSM	57.02	0.60	1.05	5.78	0.40	6.92	77.54	1.5	1.93	83.35	0.9	1.07

3.5 Numerical analysis

Numerical simulation for mechanical testing is a significant tool in materials science and engineering because it enables researchers and engineers to explore material and structure behaviour. In comparison to other materials, polymers have non-linear mechanical behaviour. As a result, standard analytical methods make it difficult to predict the behaviour of polymer-based materials, whereas FEA allows for accurate predictions. Because of its consistency and theoretical support, Finite Element Analysis (FEA) has been proposed as a more reliable method. The primary goal of this study's FEA simulation analysis is to assess the mechanical properties of 3D printed samples based on WPLA, CPLA, and FGSM under tensile and compression

loading conditions. In addition, comparing experimental results with FEA analysis allows us to replicate and evaluate the expected results from structures produced using MEX process.

The user defined ABAQUS simulation is used in this study. The meshing, geometry model, and boundary conditions are crucial components of simulation that has a big impact on output accuracy. The models are sketched as per the ASTM standards. All the parametric conditions are set equivalent with the experimentation. A computational efficient - ductile damage model is utilized. Negligible effect of porosity is considered. The critical parameters such as yield stress and initial strain are initially set to zero. Both tensile and compression tests have the following boundary conditions: Fixed displacement at one end of the sample, with symmetry boundary conditions along the sides to prevent lateral displacement. Following that, for the tensile test, there is free displacement at the opposite end of the sample, while the compression sample has fixed displacement at both ends [54]. In order to replicate a fixed boundary scenario, the required conditions are given in the coordinate system dialog box. The other end of the model is allowed to move freely along Y direction, precisely simulating the actual test conditions. Similarly, setting up a fixed boundary condition inside the mechanical category is done for the compression test. This numerical investigation selects mesh size that balances both result convergence and processing time. The mesh types of 8-node linear brick, reduced integration (C3D8R), hourglass control and 4-node 3-D (R3D4) bilinear rigid quadrilateral mesh types are used for sample (Compression and Tensile) and compression plate respectively. For the compression test, total number of mesh elements used to mesh sample and compression plate are 3500 and 592 respectively. The number of elements used in tensile sample is 4000. To model the plastic behavior of the specimen experimental stress-strain values are used.

3.5.1 Tensile characteristic analysis

Tensile characteristic results of the WPLA / CPLA and FGSM based printed samples are comprehensively presented in Fig. 5 (a, b and c). Tensile strength of the samples is obtained by 34.54, 72.90 and 56.25 MPa, respectively for the WPLA, CPLA and FGSM based printed samples.

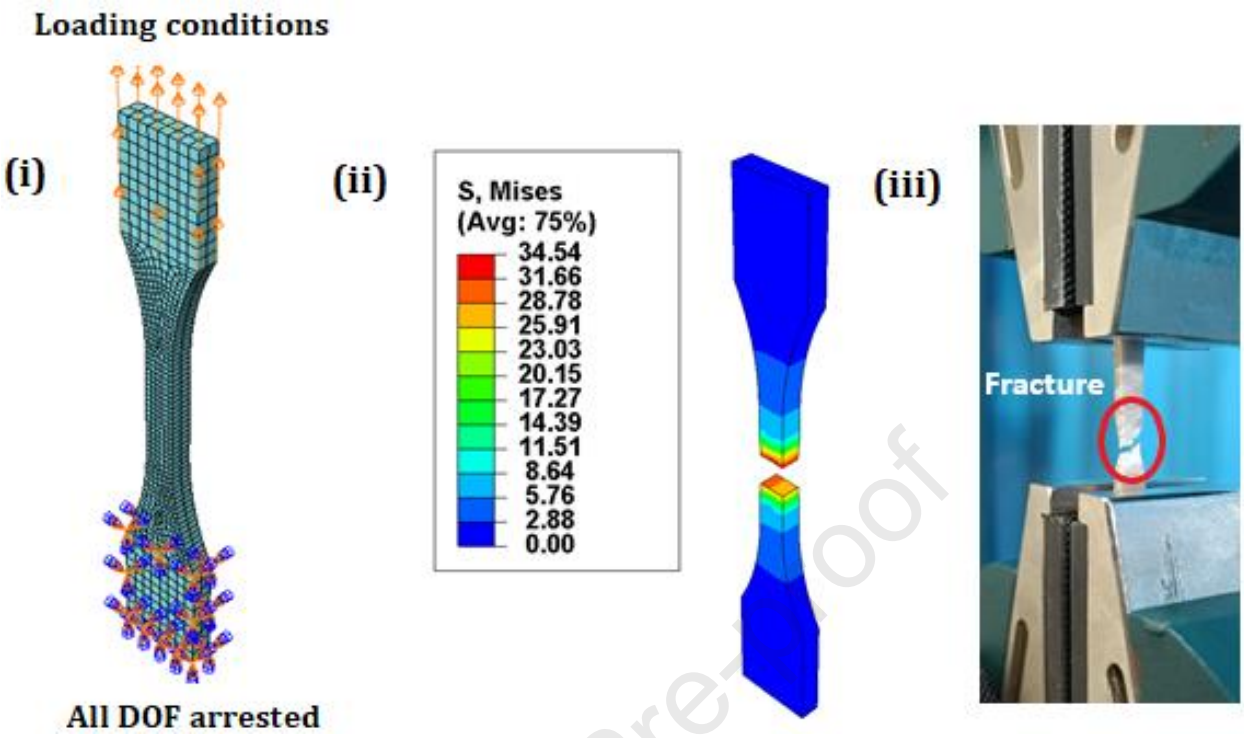

Fig. 5(a) Tensile behaviour of WPLA based sample, (i) Loading conditions on meshed sample, (ii) Numerical analysis results, (iii) Experimental view

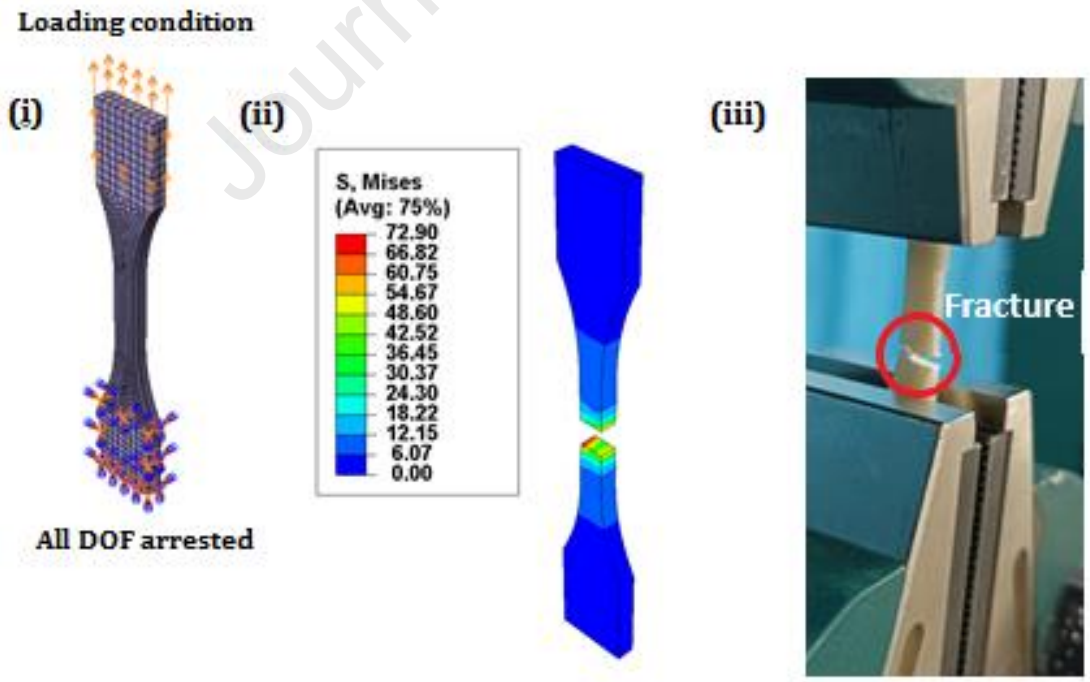

Fig. 5(b) Tensile behaviour of CPLA based sample, (i) Loading conditions on meshed sample, (ii) Numerical analysis results, (iii) Experimental view

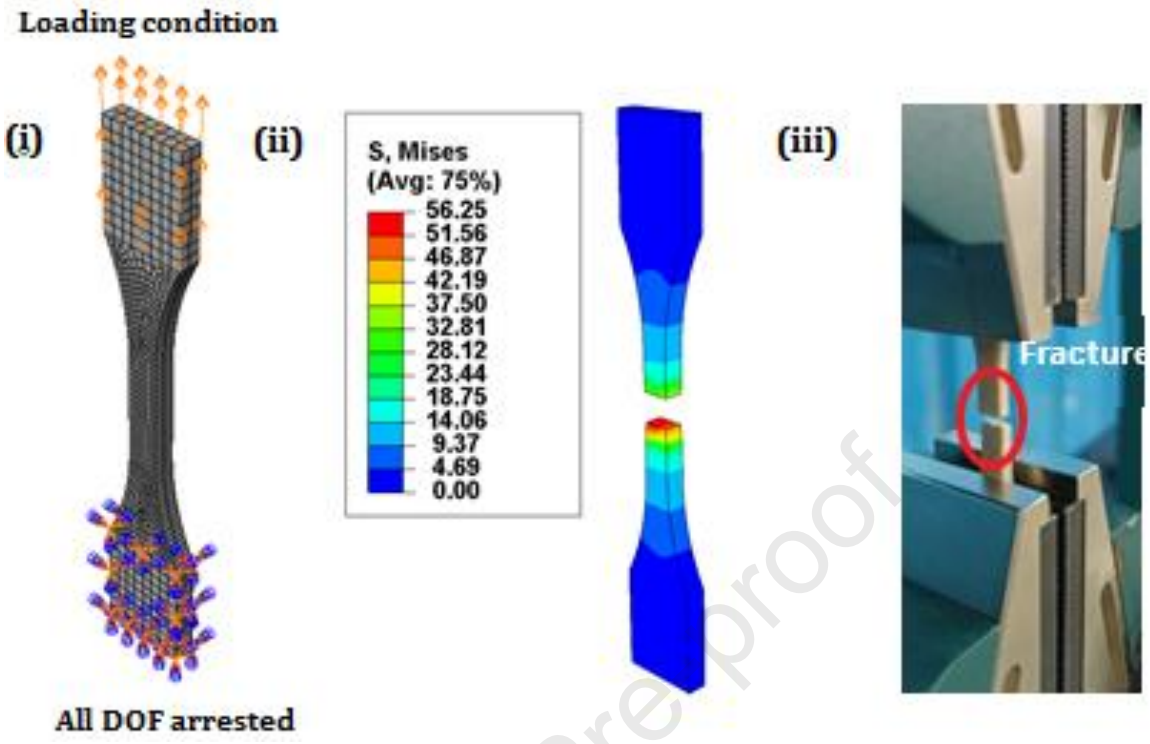

Fig. 5(c) Tensile behaviour of FGSM based sample, (i) Loading conditions on meshed sample, (ii) Numerical analysis results, (iii) Experimental view

Fig. 5(d) depicts the consolidated tensile stress-strain curve of the samples with numerical and experimental results. The obtained tensile strength of the WPLA, CPLA, and FGSM based samples from both numerical and experimental analysis are in the acceptable range, indicating that the samples' tensile behaviour is confirmed, revealing that the developed FGSM printed sample is notably a comparable material with that of the CPLA and superior to WPLA.

3.5.2 Compression characteristic analysis

The developed samples are examined with numerical analysis for assessing the compressive behaviour of the samples, similar to the tensile characteristic analysis. The compressive strength of the samples is 39.256, 98.331 and 77.495 MPa for the WPLA, CPLA, and FGSM-based samples, respectively. The compressive characteristic results of the samples are comparatively presented in Fig. 6 (a, b and c). The observed results are marginally comparable, confirming their uniform behaviour in both numerical and experimental studies.

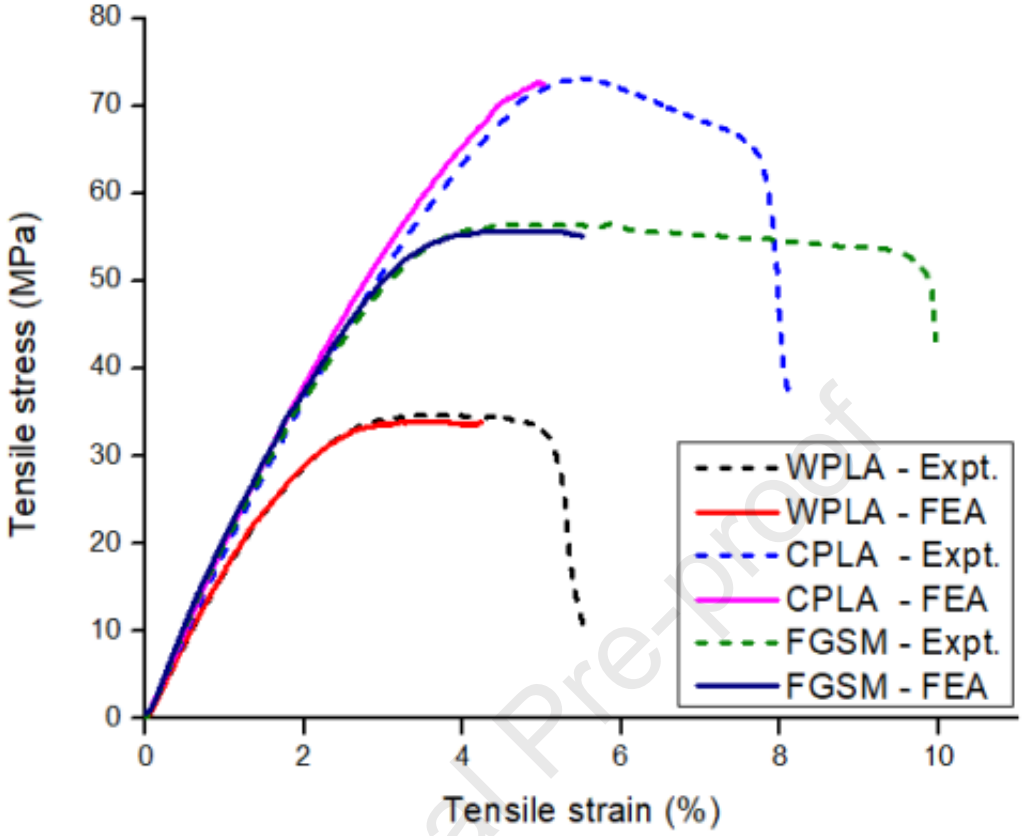

Fig. 5(d) Consolidated tensile stress – strain curve of the printed samples

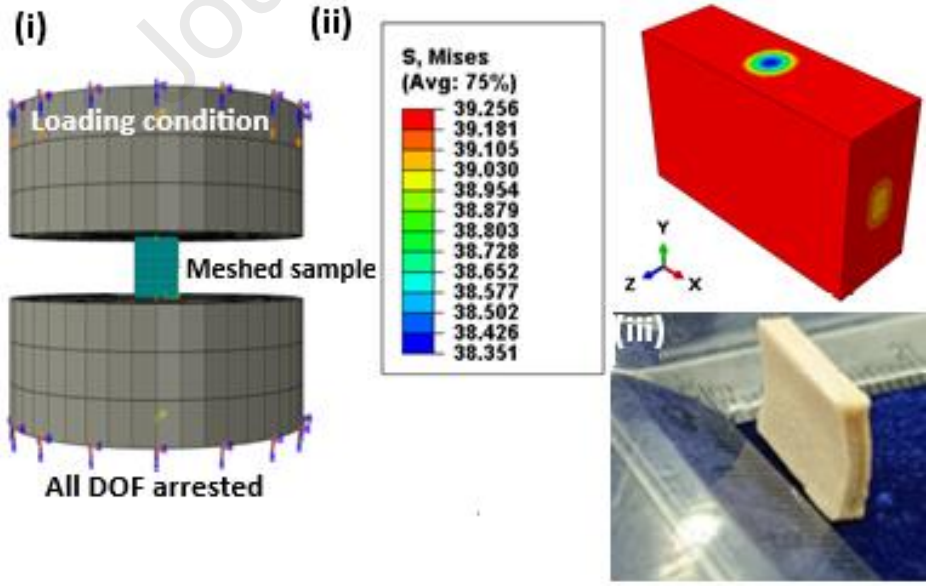

Fig. 6(a) Compressive behaviour of WPLA based sample, (i) Loading conditions on the meshed sample, (ii) Numerical analysis results, (iii) Experimental sample

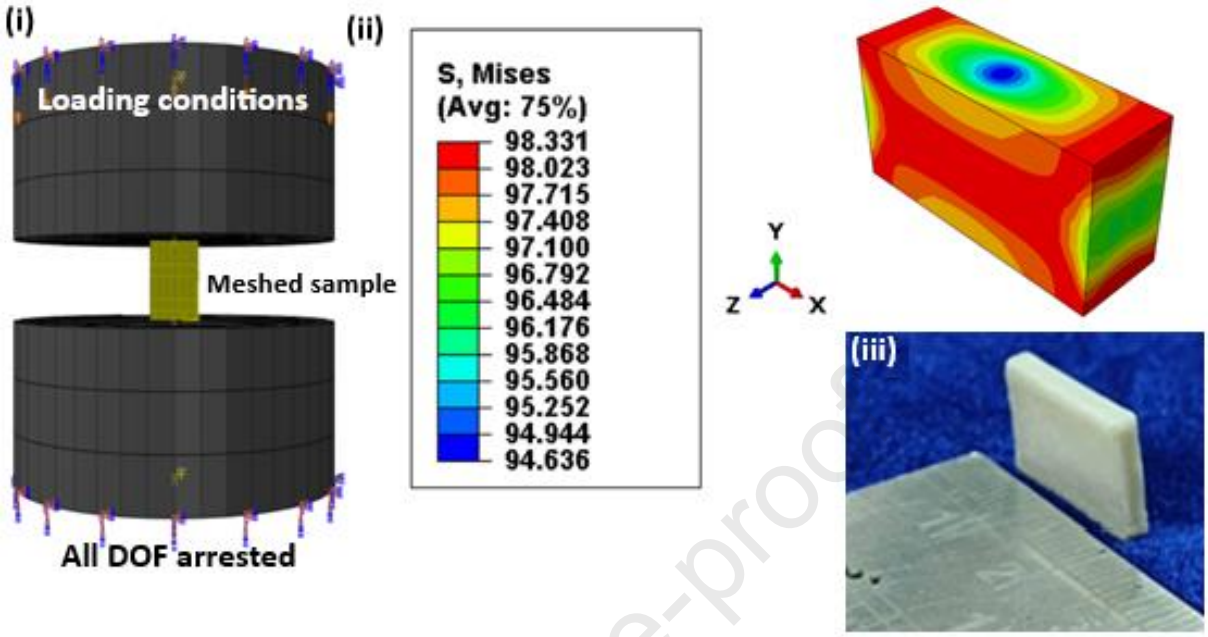

Fig. 6(b) Compressive behaviour of CPLA based sample, (i) Loading conditions on meshed sample, (ii) Numerical analysis results, (iii) Experimental sample

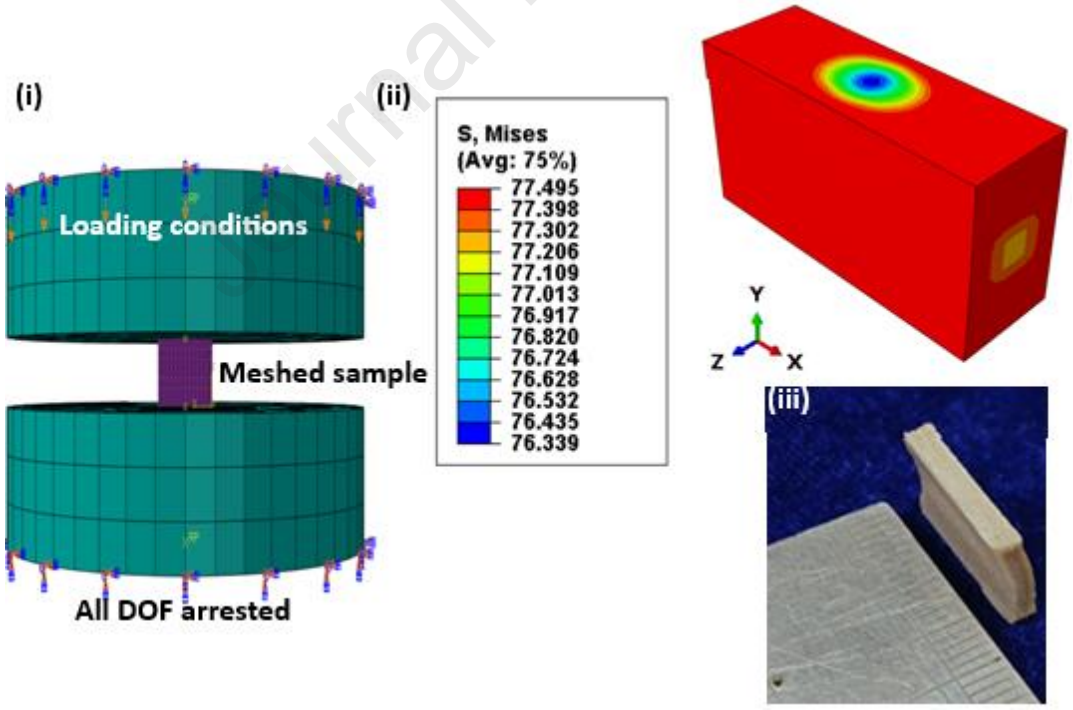

Fig. 6(c) Compressive behaviour of FGSM based sample, (i) Loading conditions on the meshed sample, (ii) Numerical analysis results, (iii) Experimental sample

As this study utilizes commercial graded filaments, the findings obtained may not be comparable with those of other grades. Although all parametric conditions are designed to be similar to experimental, negligible effect of porosity is considered for numerical studies. This could alter the mechanical characteristics of the produced composite structures in numerical studies over experimentation. In addition, the findings obtained may not be comparable with those of other grades. However, the mechanical properties of the produced FGSM have prompted researchers to develop similar FGSMs using different filament grades. The numerical model of specific commercial composite filaments attempts to investigate mechanical properties before using them in actual product manufacturing. As a result, there is a commercial advantage to developing more strengthened, reinforced polymer-based end products. Furthermore, computational results for such filaments could let researchers study various composite structures using them by predicting their mechanical properties without making them real. However, statistical analysis of experimental and numerical results is needed to confirm their reproducibility.

3.5.3 Statistical analysis of experimental and numerical results

Tensile and compression strengths of the 3D printed laminates obtained by experimental and numerical studies are statistically examined by analysing their mean (χ), standard deviation (σ) and coefficient of variation (ν). The obtained values on the statistical variables of the printed laminates are shown in Table 3.

Table 3 Statistical analysis of experimental and numerical results of printed laminates

Sample	Ultimate Tensile strength (MPa)					Ultimate Compressive strength (MPa)				
	Expt.	Numer.	χ	σ	ν (%)	Expt.	Numer.	χ	σ	ν (%)
WPLA	35.33	34.54	34.93	0.55	1.59	39.67	39.25	39.46	0.29	0.74
CPLA	73.2	72.9	73.05	0.21	0.29	98.33	98.33	98.36	0.04	0.04
FGSM	57.0	56.25	56.63	0.54	0.961	77.495	77.495	77.517	0.0318	0.041

The results revealed that the numerical studies give quite similar results compared to the experimental results, and the coefficient of variation produced is about ~1 %. It confirms their uniform tensile and compressive behaviour of the printed laminates.

3.6 Fracture morphology analysis

Fracture generally takes place as a result of the development of small voids under various loads. The fracture morphology of the failed tensile FGSM laminate is examined using SEM; the obtained image is depicted in Fig. 7.

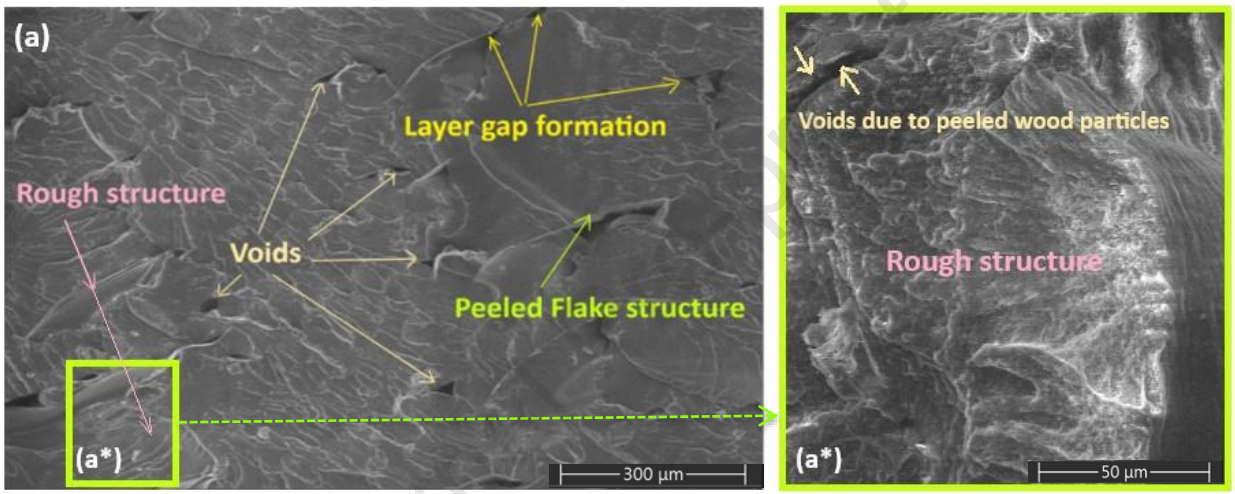

Fig. 7 Fracture morphology of the tensile fractured FGSM laminate

The existence of non-aggregated wood particles in the FGSM laminate demonstrates that the process parameters utilized during sample printing are properly selected. However, the structurally weakened flake parts of the WPLA, on the other hand, are loosened and peeled off under excessive load diminishing the composites bonding and promoting interlayer gaps and micro and macro sized voids. Existence of voids and pores as presented in composite laminate greatly reduce its mechanical stiffness and strength. Regarding, thermal modification of the wood particles is suggested which leads to decrease in pore size and overall porosity compared to non-treated wood. This is attributed to better mixing and lower interfacial energy between wood particles and PLA matrix [55]. Micro-voids appear in the outer region of the cross-section, which tends to expand as macro-voids on application of load, resulting in brittle mode of fracture. When the material fails, the accumulation of micro fractures might eventually result in a brittle macro fracture [22].

The rough surfaces shown in the morphology image (Fig. 7(a*)) of the fractured FGSM laminate represent an extended fracture. This rough fracture surface is intended to provide the sample with a small degree of elongation before failing. However, the CPLA polymer helps to improve the composites' tensile strength, which is 61.39 % higher than that of the WPLA laminate. The developed FGSM laminate's rough structure and bonding characteristics act as a barrier to fracture propagation during plastic deformation. This contributes to its brittleness, which causes failure or fracture.

3.7 Thermal properties of 3D-printed laminates

PLA, a degradable polymer, has a glass transition temperature (~58^{o}C). Below this temperature, it behaves like glass, which can creep until chilled to its transition temperature (~45^{o}C), where it becomes a brittle polymer [56]. As a result, evaluating the glass transition and associated temperatures of polymer composites is essential for confirming their potential in engineering applications. Fig. 8 depicts DSC thermograms (first heating cycle) of the WPLA, CPLA, and FGSM laminates.

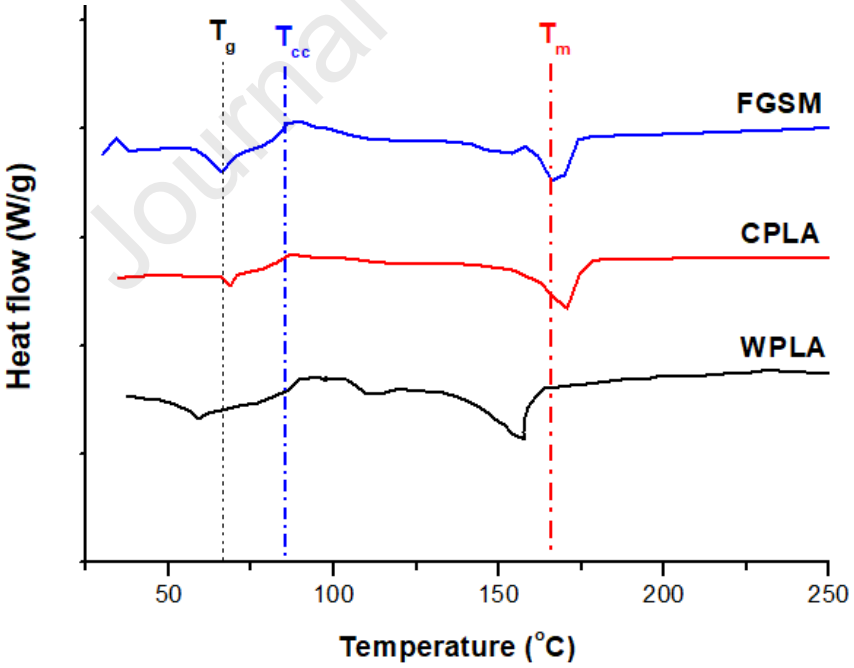

Fig. 8. DSC thermograms of 3D-printed laminates

It indicates that the glass transition temperatures (Tg) of WPLA, CPLA, and FGSM based laminates are 58.89, 68.64, and 66°C, respectively. Tg of CPLA printed laminate is higher than

that of WPLA and FGSM based laminates, owing to ceramic particle dispersion in the base PLA compound structures. Due to the presence of ceramic and wood flour particles in the FGSM laminates, the glass transition temperature is higher and merely comparable to that of WPLA and CPLA based laminates, respectively. The enhanced glass transition temperature of CPLA and FGSM based laminates makes them potential in withstanding more mechanical load which enables to produce better mechanical properties than the WPLA laminate as evidenced by the carried out mechanical characterization studies.

Furthermore, T_{cc} values of 89.84, 86.28, and 87.63°C and T_m values of 158.01, 170.64, and 166°C are obtained for the WPLA, CPLA, and FGSM based laminates, respectively. The results show that the ceramic reinforcements in the CPLA and FGSM based laminates shift the crystallization peaks to the left, making it easier to crystallize than the WPLA printed laminate. With the addition of ceramic reinforcements, heterogeneous nucleation dominates the crystallization process, which has a greater impact on the crystallization rate than that of the WPLA laminate [57]. The higher crystallization rate motivates in improving the thermal stability of the samples [58]. As a result, CPLA and FGSM based laminates exhibit greater thermal stability than WPLA laminate.

Conclusion

This comprehensive and comparative first-time attempt investigation develops a new alternate layered functionally graded structural material (FGSM) based on WPLA and CPLA polymers using the MEX process to examine its suitability for any integrated engineering applications. The developed sample is characterized in order to determine its mechanical and thermal properties and morphological structure. The mechanical properties of the developed FGSM are compared to those of printed laminates based on WPLA / CPLA polymers. The following are the key findings of the present research investigation.

- A new FGSM laminate is developed by alternate layer deposition of CPLA and WPLA polymers with appropriate process conditions of constant printing temperature (210^{o}C) and layer orientation (0^{o}).
- The tensile and compressive strength of the newly developed FGSM laminate are enhanced by 61.39 and 95.4 %, respectively than that of the WPLA laminate. When compared to the CPLA laminate, the corresponding tensile and compressive strength of the FGSM laminate

are declined by 22.1 and 21.1 %, respectively. As a result, the alternate layered FGSM laminate is superior to the WPLA and merely comparable to the CPLA based laminates.

- The uniform layer by layer deposition in the FGSM laminates aids in improving its flexural strength. It is enhanced by 107.8 % than that of the WPLA laminate. It is slightly declined by 16.39 % than that of CPLA laminate.
- The numerical studies give quite similar results compared to the experimental results, and the error percentage produced is about 1%.
- During mechanical characteristic investigations, voids are created as a result of peeled off weakened flake structures and the brittleness of the rough structure induces fractures to occur.
- DSC thermograms show that the FGSM laminate has higher glass transition (66^{o}C), cold crystallization (87.63^{o}C), and melting (166^{o}C) temperatures, indicating higher thermal stability.

Finally, it is concluded that commercial graded wood flour and ceramic-reinforced polymer composite layers establish a mechanically and thermally stable FGSM laminate which is capable of surpassing the performance constraints imposed by wood flour reinforced polymer composites. In addition to addressing current issues, these composite materials have applications in cutting-edge sectors such as automobiles, packaging, building, architecture, and construction. However, physical characteristic deviation of the composite structures in numerical and experimental models using commercial grade filaments can result in varying mechanical properties. Moreover, the results obtained are merit only for the specific commercial filaments. Hence, results from numerical and experimental studies should be confirmed by statistical analysis to ensure repeatability and a co-efficient of variation of ~1%, when examining the potential of the new functionally graded structural material utilizing various commercial grade polymer composite filaments. This research could be expanded to analyse fatigue behaviour and determine the optimum number of layer deposition for achieving maximum strength of FGSM composite structures for structural applications.

Declaration of competing interest

The authors declare that they have no known competing financial interests or personal relationships that could have appeared to influence the work reported in this paper.

Acknowledgement

This work is partially funded by Centre for Sustainable Materials and Surface Metamorphosis, Chennai Institute of Technology, India vide funding number CIT/CSMSM/2024/RP/002.

References

[1] G. Li, M. Zhao, F. Xu, B. Yang, X. Li, X. Meng, L. Teng, F. Sun, and Y. Li, Synthesis and biological application of polylactic acid, Molecules. 25/21 (2020) 5023. https://doi.org/10.3390/molecules25215023.

[2] S. Roy and J. W. Rhim, Preparation of bioactive functional poly (lactic acid)/curcumin composite film for food packaging application, Int. J. Biol. Macromol. 162 (2020) 1780-1789. https://doi.org/10.1016/j.ijbiomac.2020.08.094.

[3] Y. Liu, S. Lu, J. Luo, Y. Zhao, J. He, C. Liu, Z. Chen, X. Yu, Research progress of antistatic-reinforced polymer materials: a review, Polym. Adv. Technol. 34/4 (2023) 1393-1404. https://doi.org/10.1002/pat.5978.

[4] Q. K. Meng, M. Hetzer, and D. De Kee, PLA/clay/wood nanocomposites: nanoclay effects on mechanical and thermal properties, J. Compos. Mater. 45/10 (2011) 1145-1158. https://doi.org/10.1177/0021998310381541.

[5] A. Memarzadeh, B. Safaei, A. Tabak, S. Sahmani, C. Kizilors, Advancements in additive manufacturing of polymer matrix composites: A systematic review of techniques and properties, Mater. Today Commun. 36 (2023) 106449. https://doi.org/10.1016/j.mtcomm.2023.106449.

[6] Ramalho, D. Freitas, and H. Almeida, The anisotropy and friction effect in the design of 3D printed PLA parts–A case study, Mater. Today Proc. (2023). https://doi.org/10.1016/j.matpr.2023.08.196.

[7] W. E. Dyer and B. Kumru, Polymers as aerospace structural components: how to reach sustainability? Macromol. Chem. Phys. 224/24 (2023) 2300186. https://doi.org/10.1002/macp.202300186.

[8] M. Mani, K. W. Lyons, and S. K. Gupta, Sustainability Characterization for Additive Manufacturing, J. Res. Natl. Inst. Stand. Technol. 119 (2014) 419-428.http://dx.doi.org/10.6028/jres.119.016

[9] P. Cheng, Y. Peng, K. Wang, A Le Duigou, S Ahzi, 3D printing continuous natural fiber reinforced polymer composites: a review and outlook, Compos. B Eng. 250 (2023) 110450. https://doi.org/10.1002/pat.6242.

[10] S. M. Baligidad, A. C. Maharudresh, T. Arunkumar, K. N. Bharath, S. Abdullah, Investigation on performance of hybrid coating of hydroxyapatite and reduced graphene oxide on polyether ether ketone for orthopaedic application, Prog. Addit. Manuf. 9/2 (2024) 445-459. https://doi.org/10.1007/s40964-023-00464-1,

[11] P. Kubisa, G. Lapienis, and T. Biela, Star-shaped copolymers with PLA–PEG arms and their potential applications as biomedical materials, Polym. Adv. Technol. 32/10 (2021) 3857-3866. https://doi.org/10.1002/pat.5297.

[12] S. Maher, D. Linklater, H. Rastin, et al, Tailoring additively manufactured titanium implants for short-time pediatric implantations with enhanced bactericidal activity, Chem Med Chem. 17/2 (2022) e202100580. https://doi.org/10.1002/cmdc.202100580.

[13] Q. Lyu and S. Lu, Construction of surface HA/TiO_2 coating on porous titanium cages produced by 3D printing and the study of its efficacy in promoting the spinal fusion in a goat model, Spine J. 23/9 (2023) S109. https://doi.org/10.1016/j.spinee.2023.06.226.

[14] C. Kikuchi, F. L. S. Bussamra, M. V. Donadon, R. T. L. Ferreira, and R. C. M. Sales, Moisture effect on the mechanical properties of additively manufactured continuous carbon fiber-reinforced Nylon-based thermoplastic, Polym. Compos. 41/12 (2020) 5227-5245. https://doi.org/10.1002/pc.25789.

[15] M. T. Birosz and M. Andó, Effect of infill pattern scaling on mechanical properties of FDM-printed PLA specimens, Prog. Addit. Manuf. 9/4 (2024) 875-883. https://doi.org/10.1007/s40964-023-00487-8.

[16] P. Wang, B. Zou, S. Ding, C. Huang, Z. Shi, Y. Ma, and P. Yao, Preparation of short CF/GF reinforced PEEK composite filaments and their comprehensive properties evaluation for FDM-3D printing, Compos. B Eng. 198 (2020) 108175. https://doi.org/10.1016/j.compositesb.2020.108175.

[17] T. D. Ngo, A. Kashani, G. Imbalzano, K. T. Q. Nguyen, and D. Hui, Additive manufacturing (3D printing): A review of materials, methods, applications and challenges, Compos. B Eng. 143 (2018) 172-196. https://doi.org/10.1016/j.compositesb.2018.02.012.

[18] J. D. Kechagias and S. P. Zaoutsos, An investigation of the effects of ironing parameters on the surface and compression properties of material extrusion components utilizing a hybrid-modeling experimental approach, Prog. Addit. Manuf. (2023). https://doi.org/10.1007/s40964-023-00536-2.

[19] B. Perez, E. Celik, and R. L. Karkkainen, Investigation of interlayer interface strength and print morphology effects in fused deposition modeling 3D-printed PLA, 3D Print. Addit. Manuf. 8/1 (2021) 23-32. https://doi.org/10.1089/3dp.2020.0109.

[20] N. A. Fountas, K. Kitsakis, K.-E. Aslani, J. D. Kechagias, and N. M. Vaxevanidis, An experimental investigation of surface roughness in 3D-printed PLA items using design of experiments, Proc. Inst. Mech. Eng. J. 236/10 (2022) 1979-1984. https://doi.org/10.1177/13506501211059306.

[21] M. Mehrpouya, A. Gisario, A. Azizi, M. Barletta, Investigation on shape recovery of 3D printed honeycomb sandwich structure, Polym. Adv. Technol. 31/12 (2020) 3361-3365. https://doi.org/10.1002/pat.5020.

[22] M. K. Subramaniyan, D. Veeman, M. Vellaisamy, M. A. Browne, B. P. Patil, Manufacturing of multi material wall via fused filament fabrication: an insight characteristics, Material Science & Engineering Technology. 54 (2023) 1-9. https://doi.org/10.1002/mawe.202200293.

[23] P. Gurusamy, M. Vellaisamy, T. K. M. Kumar, M. A. Browne, S. Mohan Kumar, Some studies on functional behavior of novel multi-layered material for integrated structural application, J. Ind. Eng. Chem. 131 (2023) 545-557. https://doi.org/10.1016/j.jiec.2023.10.059.

[24] A. J. Arockiam, K. Subramanian, R. G. Padmanabhan, R. Selvaraj, D. K. Bagal, S. Rajesh, A review on PLA with different fillers used as a filament in 3D printing, Mater. Today Proc. 50 (2022) 2057-2064. https://doi.org/10.1016/j.matpr.2021.09.413.

[25] M. D. Zandi, R. Jerez-Mesa, J. Lluma-Fuentes, J. J. Roa, J. A. Travieso-Rodriguez, Int. J. Adv. Manuf. Technol. 106/9-10 (2020) 3985-3998. https://doi.org/10.1007/s00170-019-04907-4.

[26] S. Mohankumar, S. Thanigainathan, and V. Elumalai, Fabrication and mechanical behavior of structurally graded material (ceramic reinforced polylactic acid/polylactic acid) for integrated engineering application, J. Process Mech. Eng. 1-10 (2023). https://doi.org/10.1177/09544089231205791.

[27] S. Mohankumar, D. Veeman, P. Gurusamy. S. John Kennedy, B.Panda, C.Yang, Mechanical performance and microscopic characterization of additively manufactured functionally graded material (WPC/Ceramic-PLA) via fused deposition modelling, J. Process Mech. Eng. 1-10 (2023). https://doi.org/10.1177/09544089231166497.

[28] S. R. Sachin, T. K. Kannan, and R. Rajasekar, Effect of wood particulate size on the mechanical properties of PLA biocomposite, Pigment Resin Technol. 49/6 (2020) 465-472. https://doi.org/10.1108/PRT-12-2019-0117.

[29] A. Gregorova, M. Hrabalova, R. Kovalcik, and R. Wimmer, Surface modification of spruce wood flour and effects on the dynamic fragility of PLA/wood composites, Polym. Eng. Sci. 51/1 (2011) 143-150 https://doi.org/10.1002/pen.21799.

[30] R. Csizmadia, G. Faludi, K. Renner, J. Móczó, and B. Pukánszky, PLA/wood biocomposites: Improving composite strength by chemical treatment of the fibers, Compos. A. 53 (2013) 46-53. https://doi.org/10.1016/j.compositesa.2013.06.003.

[31] J. D. Kechagias, N. Vidakis, M. Petousis, N. Mountakis, A multi-parametric process evaluation of the mechanical response of PLA in FFF 3D printing, Mater. Manuf. Processes. 38/8 (2023) 941-953. https://doi.org/10.1080/10426914.2022.2089895.

[32] N. A. Fountas, S. Zaoutsos, D. Chaidas, J. D. Kechagias, N. M. Vaxevanidis, Statistical modelling and optimization of mechanical properties for PLA and PLA/Wood FDM materials, Mater. Today Proc. 93 (2023) 824-830. https://doi.org/10.1016/j.matpr.2023.08.276.

[33] N. A. Fountas, I. Papantoniou, J. D. Kechagias, D. E. Manolakos, N. M. Vaxevanidis, Modeling and optimization of flexural properties of FDM-processed PET-G specimens using RSM and GWO algorithm, Eng. Fail. Anal. 138 (2022) 106340. https://doi.org/10.1016/j.engfailanal.2022.106340.

[34] M. R. Khosravani, P. Soltani, and T. Reinicke, Fracture and structural performance of adhesively bonded 3D-printed PETG single lap joints under different printing parameters,

Theor. Appl. Fract. Mech. 116 (2021) 103087. https://doi.org/10.1016/j.tafmec.2021.103087.

[35] M. R. Khosravani, D. Anders, and T. Reinicke, Effects of post-processing on the fracture behavior of surface-treated 3D-printed parts, C.I.R.P. J. Manuf. Sci. Technol. 46 (2023) 148-156 https://doi.org/10.1016/j.cirpj.2023.08.006.

[36] N. Fountas, J. Kechagias, and N. Vaxevanidis, Statistical Modeling and Optimization of Surface Roughness for PLA and PLA/Wood FDM Fabricated Items. J. Mater. Eng. 1/1 (2023) 38-44. https://doi.org/10.61552/JME.2023.01.005.

[37] N. A. Fountas, J. D. Kechagias, S. P. Zaoutsos, and N. M. Vaxevanidis, Experimental and statistical study on the effects of fused filament fabrication parameters on the tensile strength of hybrid PLA/wood fabricated parts, Procedia Struct. Integr. 41 (2022) 638-645. https://doi.org/10.1016/j.prostr.2022.05.072.

[38] J. V. Ecker, A. Haider, I. Burzic, A. Huber, G. Eder, and S. Hild, Mechanical properties and water absorption behaviour of PLA and PLA/wood composites prepared by 3D printing and injection moulding, Rapid Prototyp. J. 25/4 (2019) 672-678. https://doi.org/10.1108/RPJ-06-2018-0149.

[39] D. Jubinville, C. Tzoganakis, and T. H. Mekonnen, Recycled PLA–Wood flour based biocomposites: Effect of wood flour surface modification, PLA recycling, and maleation. Constr. Build. Mater. 352 (2022) 129026 https://doi.org/10.1016/j.conbuildmat.2022.129026.

[40] J. A. Travieso-Rodriguez, M. D. Zandi, R. Jerez-Mesa, and J. Lluma-Fuentes, Fatigue behavior of PLA-wood composite manufactured by fused filament fabrication. J. Mater. Res. Technol. 9/4 (2020) 8507-8516. https://doi.org/10.1016/j.jmrt.2020.06.003.

[41] L. Zhang, S. Lv, C. Sun, L. Wan, H. Tan, Y. Zhang, Effect of MAH-g-PLA on the properties of wood fiber/polylactic acid composites, Polymers 9/11 (2017) 591. https://doi.org/10.3390/polym9110591.

[42] S. Guessasma, S. Belhabib, and H. Nouri, Microstructure and mechanical performance of 3D printed wood-PLA/PHA using fused deposition modeling: effect of printing temperature, Polymers 11/11 (2019) 1778. https://doi.org/10.3390/polym11111778.

[43] M. Ly, S. Spinelli, S. Hays, and D. Zhu, 3D printing of ceramic biomaterials, Engineered Regen. 3/1 (2022) 41-52. https://doi.org/10.1016/j.engreg.2022.01.006.

[44] Thomazi, C. Roman Jr, T. O. Gamba, C. A. Perottoni, and J. E. Zorzi, PLA-based ceramic composites for 3D printing of anthropomorphic simulators. Int. J. Adv. Manuf. Technol. 128/11-12 (2023) 5289-5300. https://doi.org/10.1007/s00170-023-12206-2.

[45] Z. Liu, Q. Lei, and S. Xing, Mechanical characteristics of wood, ceramic, metal and carbon fiber-based PLA composites fabricated by FDM, J. Mater. Res. Technol. 8/5 (2019) 3741-3751. https://doi.org/10.1016/j.jmrt.2019.06.034.

[46] S. Bose, D. Banerjee, A. Shivaram, S. Tarafder, and A. Bandyopadhyay, Calcium phosphate coated 3D printed porous titanium with nanoscale surface modification for orthopedic and dental applications, Mater. Des. 151 (2018) 102-112. https://doi.org/10.1016/j.matdes.2018.04.049.

[47] N. Bouamer Benrekaa and A. Younes, Characterization of polylactic acid ceramic composites synthesized by casting method, Mater. Today Proc. 42/5 (2021) 2959-2962. https://doi.org/10.1016/j.matpr.2020.12.803.

[48] H. H. Parikh, S. Chokshi, V. Chaudhary, A. Khan, and J. Mistry, Flexural response of 3D printed wood dust reinforced polymer composite, Mater. Today Proc. (2023). https://doi.org/10.1016/j.matpr.2023.06.375.

[49] N. Choudhary, V. Sharma, and P. Kumar, Reinforcement of polylactic acid with bioceramics (alumina and YSZ composites) and their thermomechanical and physical properties for biomedical application, J. Vinyl Addit. Technol. 27/3 (2021) 612-625. https://doi.org/10.1002/vnl.21837.

[50] T. Arunkumar, M. Subramaniyan, B. Prabhu, and K. Ramachandran, Development and comprehensive investigation on PLA/carbon fiber reinforced PLA based structurally alternate layered polymer composites, J. Ind. Eng. Chem. 136 (2024) 248-257. https://doi.org/10.1016/j.jiec.2024.02.012.

[51] T. Arunkumar, H. Dutta, and H. Puttaiah, Mechanical and thermal characterization of additively manufactured novel multilayer polymer composite through experiments and finite element simulation, Mech. Adv. Mater. Struct. 1–13 (2024). https://doi.org/10.1080/15376494.2024.2335654.

[52] W. Huang, H. Xu, Z. Fan, W. Jiang, and J. Liu, Dynamic failure of ceramic particle reinforced foam-filled composite lattice core, Compos. Sci. Technol. 193 (2020) 108143. https://doi.org/10.1016/j.compscitech.2020.108143.

[53] S. Palaniyappan, G. Annamalai, N. Kumar Sivakumar, and P. Muthu, Development of functional gradient multi-material composites using Poly Lactic Acid and walnut shell reinforced Poly Lactic Acid filaments by fused filament fabrication technology, J. Build. Eng. 65 (2023) 105746. https://doi.org/10.1016/j.jobe.2022.105746.

[54] X. Li, M. Ghasri-Khouzani, A.-A. Bogno, J. Liu, H. Henein, Z. Chen, A.J. Qureshi, Investigation of Compressive and Tensile Behavior of Stainless Steel/Dissolvable Aluminum Bimetallic Composites by Finite Element Modeling and Digital Image Correlation, Materials (Basel) 14/13 (2021) 3654. https://doi.org/10.3390/ma14133654.

[55] D. Krapež Tomec, M. Schwarzkopf, R. Repič, J. Žigon, B. Gospodarič, M. Kariž, Effect of thermal modification of wood particles for wood-PLA composites on properties of filaments, 3D-printed parts and injection moulded parts, Eur. J. Wood Prod. 82/2 (2024) 403–416. https://doi.org/10.1007/s00107-023-02018-2.

[56] K. Sreekumar, B. Bindhu, and K. Veluraja, Perspectives of polylactic acid from structure to applications, Polym. Renew. Resour. 12/1–2 (2021) 60–74. https://doi.org/10.1177/20412479211008773.

[57] X. Jin, X. Chen, Q. Cheng, N. W. Zhang, S. Y. Cai, and J. Ren, Non-isothermal crystallization kinetics of ramie fiber-reinforced polylactic acid biocomposite, R.S.C. Adv. 7/73 (2017) 46014–46021 https://doi.org/10.1039/C7RA09418C.

[58] C. Y. Li, F. F. Xia, L. M. Yao, H. X. Li, and X. Jia, Investigation of the mechanical properties and corrosion behaviors of Ni-BN-TiC layers constructed via laser cladding technique, Ceram. Int. 49/4 (2023) 6671–6677. https://doi.org/10.1016/j.ceramint.2022.10.104.

Conflict of Interest

The authors declare that they have no known competing financial interests or personal relationships that could have appeared to influence the work reported in this paper.